Contents lists available at ScienceDirect

Structures

journal homepage: http://ees.elsevier.com

Effects of incident angles of earthquake sequences on seismic demands of structures

Luigi Di Sarno [a], Saeed Amiri [b], Alireza Garakaninezhad [c]

[a] University of Liverpool, School of Engineering, Department of Civil Engineering and Industrial Design, UK
[b] Structural Engineering Research Center, International Institute of Earthquake Engineering and Seismology (IIEES), Tehran, Iran
[c] Department of Civil Engineering, Faculty of Engineering, University of Jiroft, Kerman, Iran

ARTICLE INFO

Keywords
Seismic excitation angle
Mainshock-aftershock sequences
SDOF systems
Constant-strength spectra

ABSTRACT

Numerous aftershocks can be triggered by a strong mainshock and may cause more severe and widespread structural damage with respect to a single seismic event. This study investigates the effect of relative differences between the incident angles of consecutive earthquakes on seismic demands of structures as bi-linear Single-Degree-Of-Freedom (SDOF) systems. To this aim, constant-strength spectra are developed based on different Normalized Engineering Demand Parameters (*NEDPs*) to identify this impact as a new seismic uncertainty. Several seismic sequences with one aftershock and also two aftershocks are generated considering different directions of both mainshocks and subsequent aftershocks as input excitations in nonlinear dynamic analyses of SDOF systems. The results demonstrate that taking into account the relative differences of the incident angles of sequential earthquakes can affect significantly seismic responses.

1. Introduction

A mainshock may trigger a cluster of aftershocks during a short time interval. Aftershocks can cause further structural and non-structural damage. Given that the current seismic codes are only based on single earthquakes [1,2], thus, considering the effects aftershocks on seismic investigations is of paramount importance. Several efforts have been directed on assessment of structures subjected to multiple earthquakes, including SDOF systems [3–7], reinforced concrete and steel frames [8–15], and existing structures that may exhibit stiffness degradation and strength reduction [16,17].

Another critical concern in Earthquake Engineering is the impact of earthquake direction on structural responses. However, numerous researchers have examined the effect of seismic incident angle on the performance of structures under single earthquakes [18–24], limited works recently have evaluated seismic behavior of different structural systems, namely SDOF systems [25], MDOF systems [26–31] against sequential earthquakes accounting for the effect of seismic incident angle. In these studies, the incident angles of consecutive earthquakes would be identical. In other words, the relative difference between successive ground motion orientations has not been considered. However, it is physically and seismologically possible to have rotated ground motion sequences. For instance, Yukutake and Lio [32] investigated the focal mechanisms of aftershocks after the Western Tottori Earthquake occurred in 2000. They showed that the aftershocks around the mainshock fault were distributed within zones of 1.0–1.5 km in thicknesses, and also their focal mechanisms were significantly diverse.

The objective of this paper is to reveal the effect of the relative difference between incident angles of mainshock and subsequent aftershocks, as a new seismic uncertainty, on nonlinear seismic responses of structures as SDOF systems. For this purpose, after generating mainshocks and aftershocks with various incident angles, constant-strength spectra based on different Normalized Engineering Demand Parameters (NEDPs) are developed. Furthermore, seismic sequences including one aftershock and also two aftershocks are considered in this regard.

2. Methodology

The epicenter location is not certainly determined before the occurrence of an earthquake, thus the direction of ground motion with respect to the orientation of a structure is not identified as a priori. Hence, one of the most important uncertainties in the process of determining the structural damage is the orientation of the earthquake record. Additionally, there are no specific and detailed provisions about determining the most critical direction of earthquake excitation in current seismic regulations. This can lead to more unreliable seismic design and assessment of structures. Moreover, this concern is more complicated regarding consecutive earthquakes, since multiple incident angles can exist corresponding to each ground motion as shown in Fig. 1. In this figure, three successive ground motions, denoted by GM_1, GM_2, and GM_3 are rotated by different angles of θ_1, θ_2, and θ_3, respectively. In other words, aftershocks, generated by slip distributions on the fault plane, are typically characterized by their epicenter, which does not necessarily coincide with that of the mainshock [32]. In addition, in Fig. 1, x and y represent principal axes of a structure, while x' and y'

E-mail addresses: luigi.di-sarno@liverpool.ac.uk (L. Di Sarno); a.garakani@ujiroft.ac.ir (A. Garakaninezhad)

https://doi.org/10.1016/j.istruc.2020.09.064
Received 4 July 2020; Received in revised form 23 August 2020; Accepted 26 September 2020
Available online xxx
2352-0124/

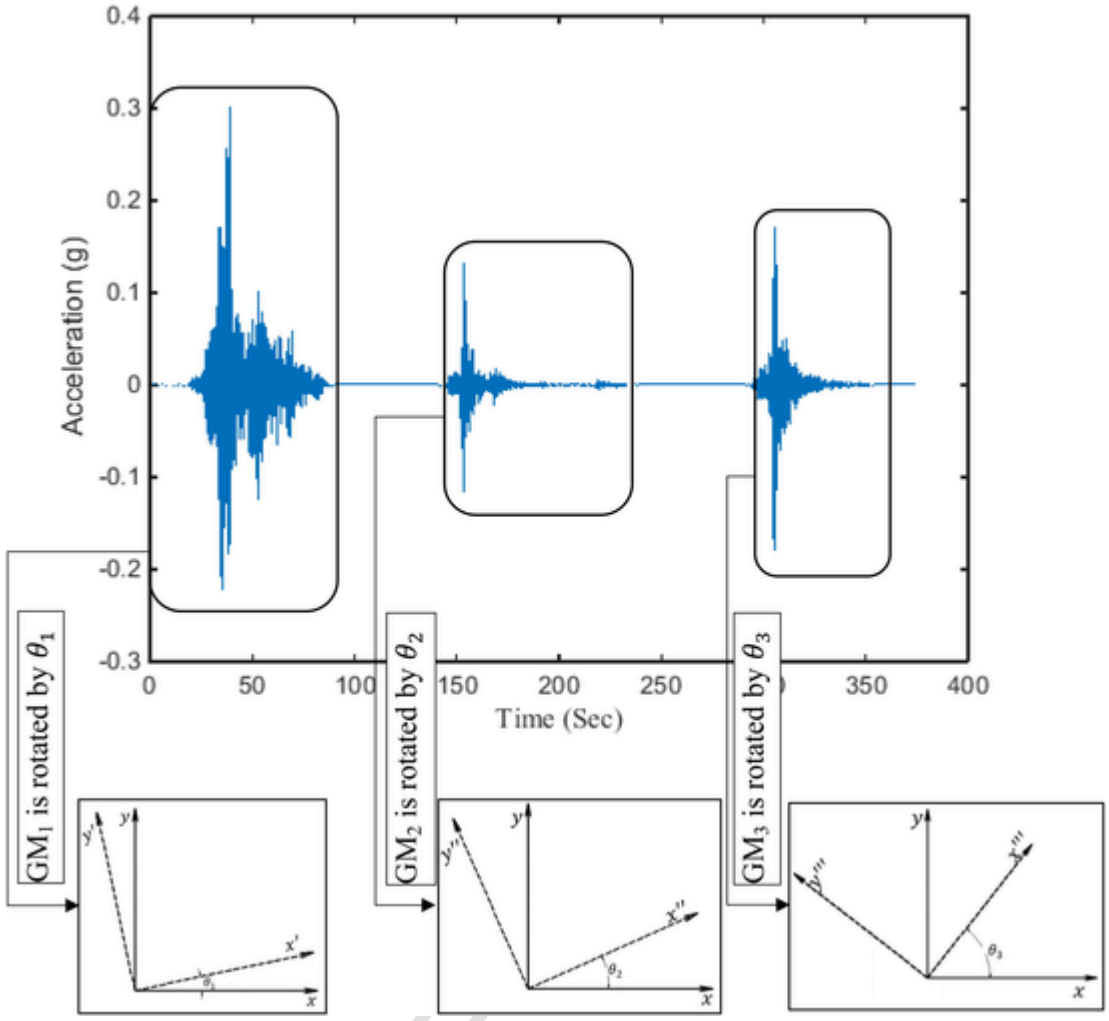

Fig. 1. Seismic incident angles of consecutive earthquakes.

are mainshock axes, x'' and y'' stand for the first aftershock axes, and x''' and y''' denote the second aftershock axes. In fact, there is only one ground motion incident angle parameter in the case of single earthquake, i.e. mainshock, but there are at least two parameters associated with ground motion incident angle, one related to mainshock and another related to subsequent aftershock, for multiple earthquakes. It is noted that the number of earthquake incident angle parameter will be more than two parameters, if the number of aftershocks is more than one, or as the number of sequences increases. Thus, it is necessary to rotate all n successive shocks to consider the effects of seismic incident angles on structural responses. In this way, each shock is rotated by θ_i, $i = 1, 2, \ldots, n$, such that this angle is not necessary equal throughout the sequence. That is, each motion, including mainshock or aftershock, can be rotated by a different angle. The flowchart indicated in Fig. 2 describes the generation of rotated multiple earthquakes, so that each shock is applied to structures with a specific angle.

In this paper, two and three successive motions, including sequences with one mainshock and one aftershock and also one mainshock and two aftershocks are taken into account, then any of them is rotated with the increment of 45° for the brevity and simplicity of the computations and results. Hence, mainshock, the first aftershock and the second one are rotated from their initial orientation by angles θ_m, θ_{a1} and θ_{a2} respectively, such that these angles are not necessarily identical with respect to each other. Therefore, each rotated input seismic sequence for dynamic analyses includes a mainshock rotated by the angle of incidence of θ_m, a time-gap (50 s) having zero acceleration ordinates to rest of the structure, the first aftershock rotated by the angle of θ_{a1}, a time-gap of 50 s, and the second aftershock rotated by the angle of θ_{a2}. As mentioned, various incident angles are considered for mainshocks and subsequent aftershocks, namely $\theta m, \theta a1, \theta a2 = 0°, 45°, 90°, 135°, 180°$. Thus, $5 \times 5 \times 5 = 125$ rotated sequences are generated, when there are one mainshock and two aftershocks.

In order to quantify the effect of the relative differences of the incident angles of mainshock and subsequent aftershocks, namely when $\theta_m \neq \theta_{a1}$, θ_{a2}, on the structural performance, the Normalized Engineering Demand Parameter (*NEDP*) is considered. Hence, for each value of $\theta m, \theta m = 0°, 45°, 90°, 135°, 180°$, this parameter ($NEDP_\theta$) at various θ_{a1} and θ_{a2} are computed using Eq. (1).

$$NEDP_\theta = \frac{EDP_\theta}{EDP_0} \tag{1}$$

where EDP_θ is responses of structures against seismic sequences at angles of $\theta a1, \theta a2 = 0°, 45°, 90°, 135°, 180°$ when $\theta_m \neq \theta_{a1}$, θ_{a2}, and EDP_0 stands for seismic responses when the differences between the mainshock and subsequent aftershocks incident angles are zero, i.e. $\theta_m = \theta_{a1} = \theta_{a2}$. Therefore, in the case of two-sequence earthquakes, EDP_0 shows when the incident angle of aftershock is equal to that of mainshock. Similarly, for three-sequence earthquakes, EDP_0 is seismic response of structures, when the angles of both aftershocks equal the mainshock angle.

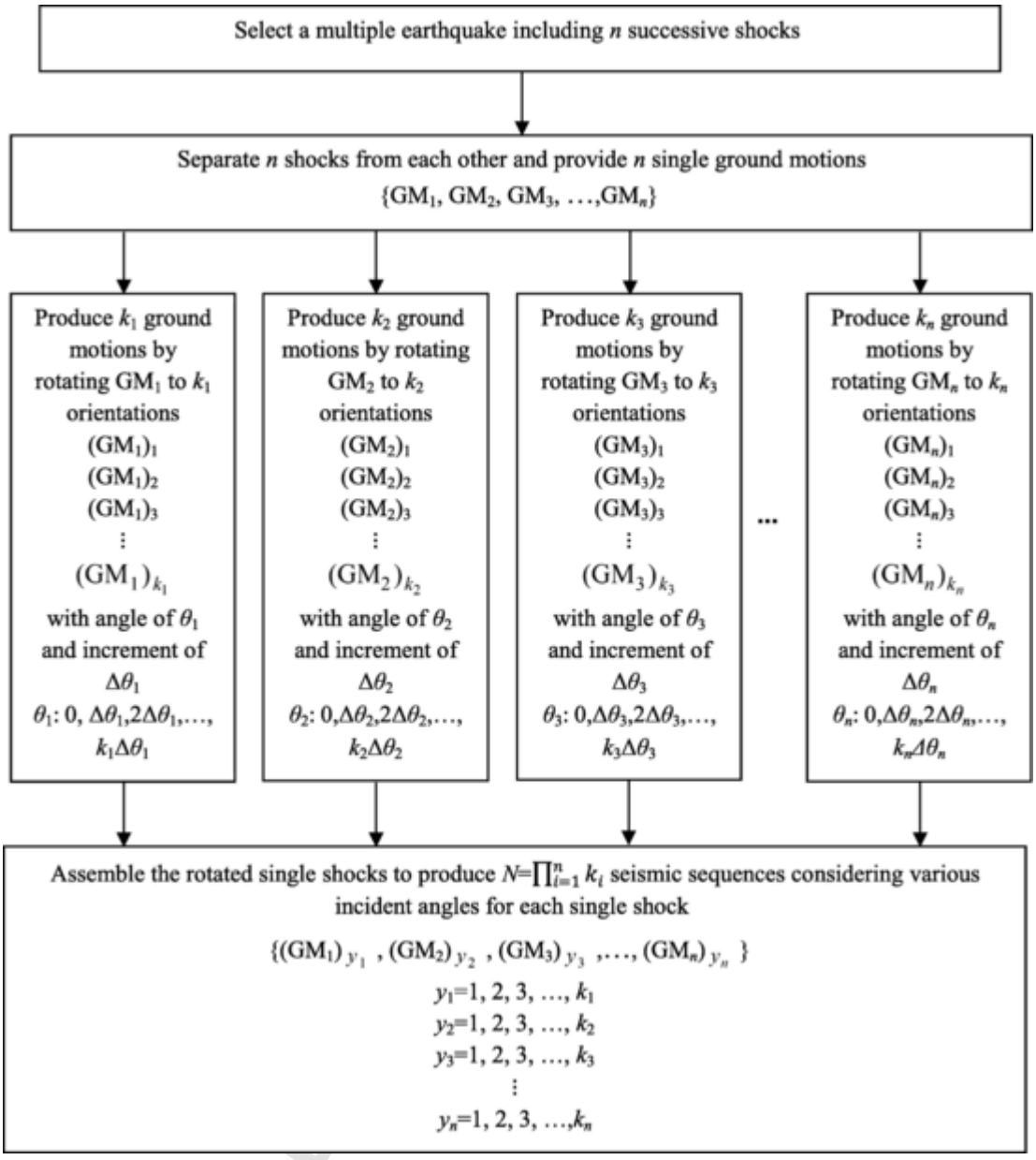

Fig. 2. Flowchart showing the methodology for generating rotated multiple earthquakes.

3. Structures and seismic sequences

3.1. Structures

The current paper aims to introduce the additional parameters induced by the rotation of successive earthquakes, as discussed in Section 2, for SDOF systems with the elastic-perfectly-plastic model, as a preliminary study to investigate the effect of this new seismic uncertainty on nonlinear responses. However, different hysteresis models can be used in this regard, as indicated in [33–38] for better investigations, which will be considered in further research works. It is noted that in order to compute seismic responses of SDOF systems in different angles in the horizontal plane, the well-known transformation is used, which is employed in [22,39]:

$$\begin{aligned} x_a &= GM_x \cos\theta + GM_y \sin\theta \\ y_a &= -GM_x \sin\theta + GM_y \cos\theta \end{aligned} \tag{2}$$

where θ, including θ_m, θ_{a1} and θ_{a2}, stands for the incident angle of earthquake, presented in the previous section, GM_x and GM_y denote the accelerogram components of the un-rotated records.

The constant-strength spectra are developed for all combinations of mainshock and subsequent aftershock incident angles, considering the variations of the natural vibration period (T), T = 0.1–2.8 s with a step of 0.3 s, and also the strength reduction factor (R), R = 2, 4, 6. Three different *EDPs* are extracted to identify the seismic performance of structures: (a) maximum inelastic displacement, *MD*, as a widely accepted seismic demand in practical issues; (b) maximum inelastic absolute acceleration, *MA*, which is appropriate for assessing of non-structural elements; and (c) normalized hysteretic energy, *NHE*, as an effective representative of cumulative structural damage, which is expressed as Eq. (3).

$$NHE = \frac{E_H}{F_y D_y} \tag{3}$$

where E_H denotes the hysteretic energy dissipation of an inelastic structure, F_y and D_y stand for the yield strength and the yield displacement.

It is noted that each *EDP* is normalized according to Eq. (1), to quantify the effect of the relative differences of the incident angles of consecutive earthquakes on structural performance.

3.2. Seismic sequences

Two sets of real mainshock-aftershock sequences from the California region, including Imperial Valley, Livermore, Whittier Narrows, Mammoth Lakes, Coalinga, Chalfant Valley, Northridge, as well as Chi-Chi earthquakes, with one aftershock and also two aftershocks, are employed as seed earthquakes to generate rotated seismic sequences. Each set includes 10 seismic sequences, totally 20 mainshock-aftershock sequences. The ground motions are gathered from the Pacific Earthquake Engineering Research (PEER) [40], by satisfying these criteria: (a) two horizontal components should be accessible for a given station; (b) moment magnitude (M_w), is greater than or equal to 5.0; (c) average horizontal peak ground acceleration (*PGA*) is greater than or equal to 0.04 g; (d) average horizontal peak ground velocity (*PGV*) is greater than or equal to 1.0 cm/sec; (e) average shear-wave velocity in the uppermost 30 m (VS_{30}), is within 100 and 1000 m/s; (f) closest site-to-fault-rupture distance is less than 75 km, and (g) recording station is at free field or in light construction.

As mentioned in Section 2, five different angles are considered for either mainshock or aftershock/aftershocks, $\theta m, \theta a1, \theta a2 = 0°, 45°, 90°, 135°, 180°$. Thus, for each multiple earthquakes, with one mainshock and one aftershock, there are $5 \times 5 = 25$ rotated ground motions, while in the case of sequences including one mainshock and two aftershocks, $5 \times 5 \times 5 = 125$ rotated records are generated for each sequence. Hence, $10 \times 25 = 250$ records are used as two-sequence earthquakes and $10 \times 125 = 1250$ records are also employed as three-sequence ground motions. As a result, $250 + 1250 = 1500$ seismic sequences are considered in this work.

4. Statistical results

After carrying out nonlinear time history analyses of the structures under mainshock-aftershock sequences rotated to various angles, the normalized responses, i.e. $NEDP_\theta$ for three different *EDPs*, stated in sub-section 3.1, are computed using Eq. (1). Only some results are presented in this Section for the sake of brevity of the paper. The maximum value of normalized responses, $NEDP_\theta$, for all combinations of incident angles of mainshocks and subsequent aftershocks, namely 25 and 125 combinations of θ_m, θ_{a1} and θ_{a2} for two-sequence and three-sequence earthquakes, respectively, are obtained for each ground motion. Then the mean value of them for 10 sequences including one aftershock and also those having two aftershocks are shown in Figs. 3 and 4, respectively. The figures situated on the left side, namely Fig. 3(a), 4(a), Fig. 3(c), 4(c) and Fig. 3(e), 4(e) indicate the mean maximum $NEDP_\theta$. Moreover, the SDOF system with $R = 2$ is taken into account as the reference structural model for better comparison of $NEDP_\theta$ in the structures with different R values over the vibration period range considered. Therefore, the figures located on the right side, namely Fig. 3(b), 4(b), Fig. 3(d), 4(d) and Fig. 3(f), 4(f) show the difference $NEDP_\theta$ between the systems with $R = 2$ and those having $R = 4$ and $R = 6$. This parameter is represented by $DNEDP_\theta$ in these figures, thus, $(DNEDP_\theta)_4 = (NEDP_\theta)_{R=2} - (NEDP_\theta)_{R=4}$, and $(DNEDP_\theta)_6 = (NEDP_\theta)_{R=2} - (NEDP_\theta)_{R=6}$.

A glance at Fig. 3, provided for sequences with one mainshock and one aftershock, reveals when the directions of mainshocks and aftershocks would be different, $\theta_m \neq \theta_{a1}$, the values of the *EDPs* can be significantly higher than the case of $\theta_m = \theta_{a1}$, i.e. $NEDP_\theta > 1$. According to Fig. 3(a), 3(c) and 3(e), $NEDP_\theta$ for all values of T considered in this study, and also for three types of demands, is greater than one, such that its value for *MD* in the case of stiffer structures ($T \leqslant 0.7$ s) with $R = 2$ reaches approximately 2.15 on average (see Fig. 3(a)). This means when $\theta_m \neq \theta_{a1}$, seismic responses can rise considerably by 115% with respect to the case of $\theta_m = \theta_{a1}$. However, in these systems, the normalized *MD* declines, as R increases. The average value of which is about 1.58 for both $R = 4$ and 6. In addition, $NEDP_\theta$ of maximum displacement would be 1.27 on average for $T \geqslant 1.0$ s and three values of R. In view of Fig. 3(c), $NEDP_\theta$ average value for *MA* is just over 1.16. Moreover, the average normalized response computed due to *NHE* for short-to-moderate period structural systems ($T \leqslant 1.6$ s) possessing $R = 2$ is roughly 1.4 (see Fig. 3(e)), which indicates the value of *NHE* can see a rise of 40% when the incident angles of mainshock and aftershock are not identical, compared to the situation that they are equal with one another. On the other hand, these structures having $T > 1.6$ s experience a constant value of $NEDP_\theta$, such that it is around 1.25. Moreover, the mean normalized response almost follows a stable trend for larger R ($R = 4$ and 6), reaching about 1.34 for all values of T considered. Furthermore, Fig. 3(b), 3(d) and 3(f) confirm when T tends to increase, the effect of R on $NEDP_\theta$ would be minor, so that $(DNEDP_\theta)_4 \approx (DNEDP_\theta)_6$ for long-period systems. These differences also converge to zero for these structures. However, the values of $(DNEDP_\theta)_4$ and $(DNEDP_\theta)_6$ in Fig. 3(d) are close to zero throughout the period range, such that the absolute maximum their value is nearly 0.12. It can be concluded that the *EDPs* of long-period structures can be affected slightly, when $\theta_m \neq \theta_{a1}$ compared with $\theta_m = \theta_{a1}$.

As mentioned previously, Fig. 4 delineates the mean inelastic spectra in terms of three different *EDPs* under sequences including one mainshock and two aftershocks. It can be observed that the presence of the relative differences between successive incident angles ($\theta_m \neq \theta_{a1}$, θ_{a2}) can lead to increase of responses ($NEDP_\theta > 1$). According to Fig. 4(a), maximum displacement of structures (*MD*) faces at least a marked rise of 30% ($NEDP_\theta > 1.3$) for all values of R. In addition, the average normalized *EDP* for short-to-moderate period structural systems ($T \leqslant 1.0$ s) with $R = 2$ is approximately 1.74. This reveals that these structures are more sensitive to the differences between incident angles under multiple earthquakes. The mean $NEDP_\theta$ sees a sudden fall as the vibration period increases, reaching just above 1.41 in the range of $T \geqslant 1.3$ s. Furthermore, when R tends to rise ($R = 4$ and 6), the variation of $NEDP_\theta$ decreases to a great extent, so that its value would be 1.57 throughout the period range (0.1 s $\leqslant T \leqslant$ 2.8 s).

In view of Fig. 4(c), the normalized response based on the *MA* witnesses an almost constant trend over the period variety considered, exceeding 1.23 on average for all three values of R. Moreover, Fig. 4(e) shows if $\theta_m \neq \theta_{a1}$, θ_{a2}, SDOF systems having $T = 1.0$ s as well as $R = 2$ experience seismic damage in terms of *NHE* which can be 80% more than the situation of $\theta_m = \theta_{a1} = \theta_{a2}$, i.e. $NEDP_\theta = 1.8$. This parameter declines rapidly, as the strength reduction factor (R) goes up, reaching a stable value of 1.3 for all vibration periods. Additionally, Fig. 4(b), 4(d) and 4(f) delineate the long-period region is not significantly sensitive to $NEDP_\theta$, and the values of $(DNEDP_\theta)_4$ and $(DNEDP_\theta)_6$ move to zero in this region. Also, the effect of R is not important on MA in comparison with the other demands, so that the absolute maximum of $(DNEDP_\theta)_4$ and $(DNEDP_\theta)_6$ would be 0.15 for all period values (see Fig. 4(d)). As a result, Figs. 3 and 4 demonstrate short-period structures can be vulnerable against seismic sequences, when the incident angles of mainshock and subsequent aftershocks are not identical. It is noted that short-period structures have been traditionally referred to as the ones having $T < 0.7$ s. However, it appears that there is a lack of theoretical background for such an assumption in the technical literature. Additionally, further studies are being conducted with a series of constitutive laws, thus it seems reasonable to stress the current limit of this investigation in the paper. Although, based on the outcomes of the numerical investigation, the present approach can be extended to the N2 method (equal energy period range) [41].

Polar diagrams are also employed to represent the variations of $NEDP_\theta$ at various incident angles. To this aim, the changes of this ratio for three seismic demands (*MD*, *MA*, *NHE*) are depicted in Fig. 5 for a

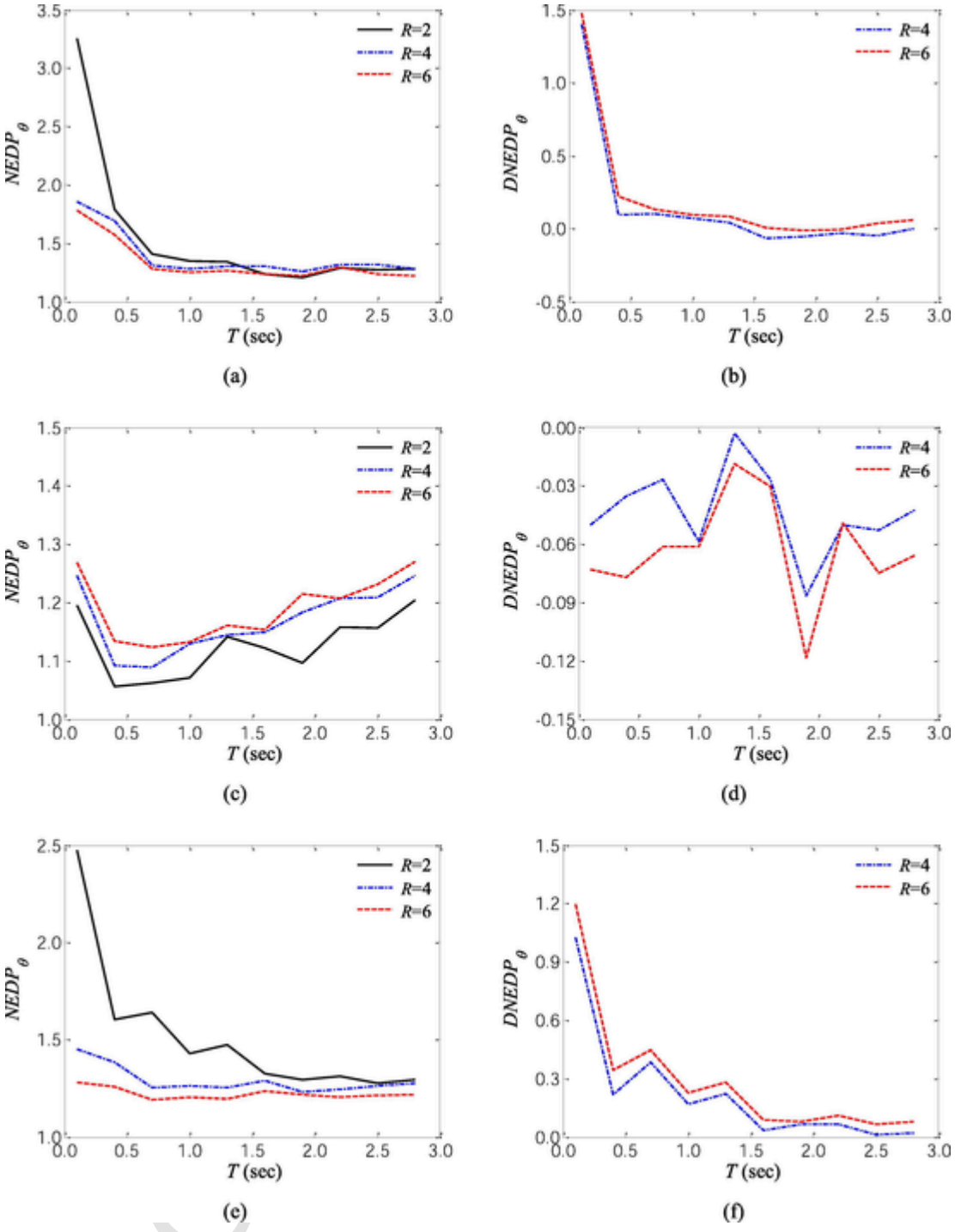

Fig. 3. Mean inelastic spectra in terms of $NEDP_\theta$ and $DNEDP_\theta$ under sequences with one aftershock for (a), (b). *MD*; (c), (d). *MA*; and (e), (f). *NHE*.

typical SDOF system, with $T = 1.3$ s and $R = 4$, under the Livermore sequence including one mainshock and one aftershock, when the angle of aftershock is varied, namely $\theta a1=0°,45°,90°,135°,180°$ and the angle of mainshock is equal to $90°,135°$, i.e. $\theta m=90°,135°$. These combinations ($\theta m=90°,\theta a1$) and ($\theta m=135°,\theta a1$) are selected from existing 25 combinations of θ_m and θ_{a1}, because the normalized response due to them is more than one, as shown in Fig. 5(a) and Fig. 5(b), respectively. It is useful to depict $NEDP_\theta$ over $0°$ to $360°$ by reflection in Fig. 5. The $NEDP_\theta$ due to the maximum displacement, *MD*, is 1.87 at $\theta m=90°$ and $\theta a1=0°$ (Fig. 5(a)). Additionally, this parameter reaches 1.25, when $\theta m=135°$ and $\theta a1=0°$(Fig. 5(b)). As seen in Fig. 5, the maximum $NEDP_\theta$ for the other demands, *MA* and *NHE*, can occur in different angles. This figure shows if the directions of mainshock and subsequent aftershock would be different ($\theta_m \neq \theta_{a1}$), more critical structural responses can be obtained.

Similarly, for the same oscillator ($T = 1.3$ s and $R = 4$), the changes of $NEDP_\theta$ at different angles of combinations the second aftershock (θ_{a2}), varied from $0°$ to $180°$, in a sequence with two aftershocks, Coalinga earthquake, when $\theta m=90°,\theta a1=135°$ and $\theta m=135°,\theta a1=90°$ are presented in Fig. 6(a) and (b), respectively. The combinations ($\theta m=90°,\theta a1=135°$ and

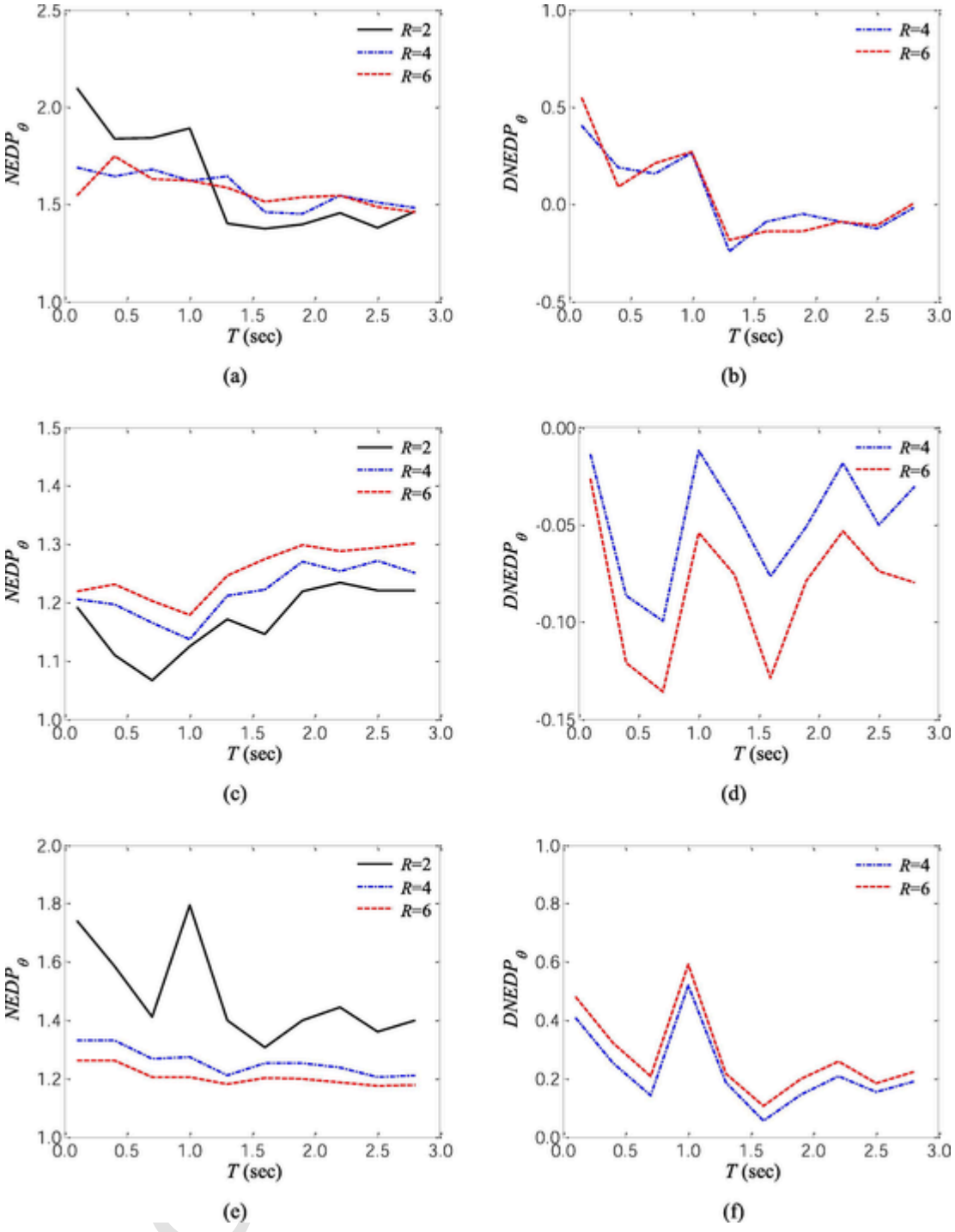

Fig. 4. Mean inelastic spectra in terms of $NEDP_\theta$ and $DNEDP_\theta$ under sequences with two aftershocks for (a), (b). *MD*; (c), (d). *MA*; and (e), (f). *NHE*.

$\theta m=135°, \theta a1=90°$) are considered from existing 125 combinations of θ_m, θ_{a1} and θ_{a2}, since in which the maximum value of $NEDP_\theta$ is considerable. According to Fig. 6(a), *MD* can rise by about 38% at $\theta a2=0°$ in comparison with the case of $\theta m=\theta a1=\theta a2=90°$, namely $NEDP_\theta = 1.38$. This increase for both *MA* and *NHE* occurs at $\theta a2=45°$, such that it is around 12% and 20% for these demands, respectively. Furthermore, a similar trend is observed in Fig. 6(b), so that $NEDP_\theta$ can see its maximum value at 1.58 for *MD*, when $\theta a2=0°$. These figures denote if consecutive ground motions are applied to the structure with different orientations ($\theta_m \neq \theta_{a1} \neq \theta_{a2}$), higher responses can be resulted in, compared to the case of $\theta_m = \theta_{a1} = \theta_{a2}$.

5. Summary and conclusions

This study investigates the effect of the relative differences between successive incident angles on various seismic responses of nonlinear structures. To this aim, structures as SDOF systems are taken into account with a variety of T and R. Moreover, a methodology to generate rotated seismic sequences is presented. Then constant-strength spectra are developed under rotated mainshock-aftershock sequences including one aftershock and two aftershocks, rotated to various angles, from $0°$

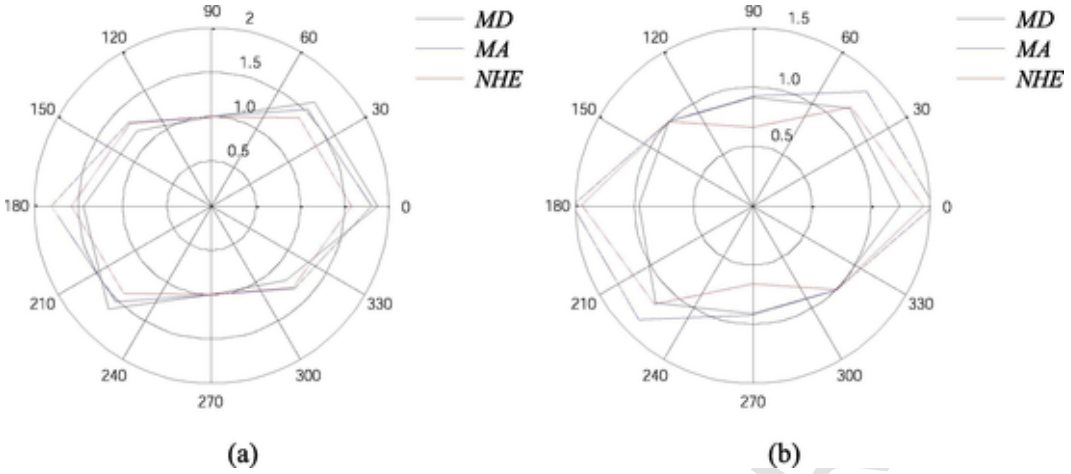

Fig. 5. Polar diagrams in terms of the normalized response under sequences with one aftershock, when (a). $\theta m=90°$; (b). $\theta m=135°$.

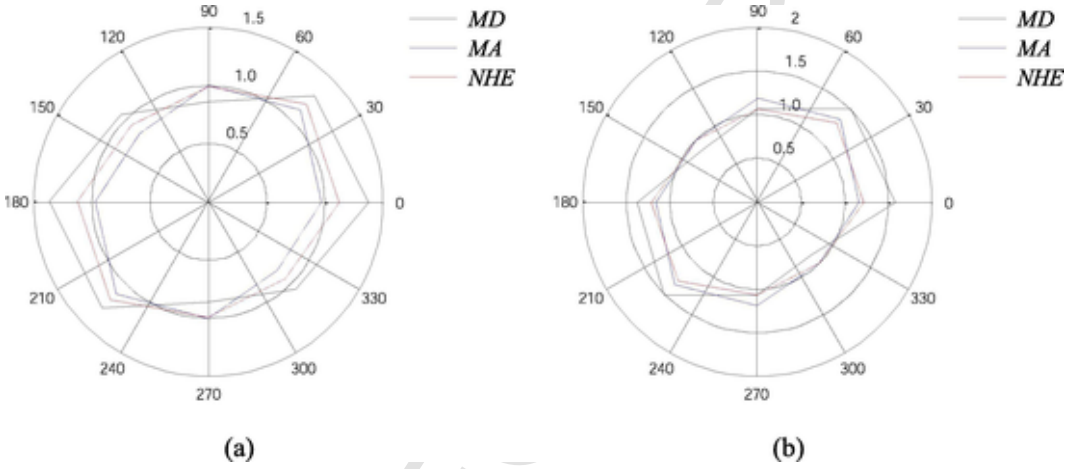

Fig. 6. Polar diagrams in terms of the normalized response under sequences with two aftershocks, when (a). $\theta m=90°$, $\theta a1=135°$; (b). $\theta m=135°$, $\theta a1=90°$.

to $180°$, such that the angles of consecutive ground motions are not necessarily identical. In other words, θ_m, θ_{a1}, and θ_{a2} can be different with respect to each other. Three EDPs of nonlinear structures are extracted at different combinations of θ_m, θ_{a1} , and θ_{a2}. After that, for each value of θ_m, the responses are normalized to when $\theta_m = \theta_{a1} = \theta_{a2}$ at various θ_{a1} and θ_{a2} to quantify the impact of different directions of mainshock and subsequent aftershock/aftershocks on structural behavior. Afterwards, the mean maximum normalized responses, $NEDP_\theta$, of all existing combinations of mainshock and aftershock incident angles, for two-sequence and three-sequence earthquakes considered in this paper are computed. The main conclusions of this paper are summarized as follows.

(a) Short-period structures ($T \leqslant 0.7$ s) with $R = 2$ can experience much more seismic damage under multiple earthquakes, including one mainshock and one aftershock, if there is a relative difference between incident angles of mainshock and subsequent aftershock. For instance, when $\theta_m \neq \theta_{a1}$, the maximum displacement, *MD*, of these systems can increase approximately 115% on average, with respect to the case of $\theta_m = \theta_{a1}$. Moreover, the average value of the normalized *MD* of these structures, $NEDP_\theta$, would be about 1.58 for higher R (4 and 6). The values of $NEDP_\theta$ for the other demands, *MA* and *NHE*, are also more than one for all three R values throughout the period range considered. It is worth noting that the present approach can be extended to the N2 method (equal energy period range).

(b) For sequences with two aftershocks, the normalized response in terms of *MD* can exceed 1.3 ($NEDP_\theta$>1.3) for all values of R. In addition, the average value of this ratio for short-to-moderate period structural systems ($T \leqslant 1.0$ s) having $R = 2$ is about 1.74. The $NEDP_\theta$ based on the *MA* can see an almost constant trend over the period variety considered, reaching 1.23 on average for all three values of R. Moreover, in the case of $\theta_m \neq \theta_{a1}$, θ_{a2}, SDOF systems with $T = 1.0$ s and R = 2 would face the rise of *NHE* which can be 80% more than the situation of $\theta_m = \theta_{a1} = \theta_{a2}$, i.e. $NEDP_\theta = 1.8$.

(c) Polar diagrams are presented for an oscillator with $T = 1.3$ s and $R = 4$, under the Livermore sequence including one mainshock and one aftershock, and also under the Coalinga sequence with one mainshock and two aftershocks. The observations prove that the normalized maximum displacement can reach 1.87 at $\theta m=90°$ and $\theta a1=0°$ for the two-sequence earthquake. Furthermore, in the case of the three-sequence earthquake, this demand increases by almost 38% at $\theta m=90°$,$\theta a1=135°$, and $\theta a2=0°$. The maximum $NEDP_\theta$ for the other demands, *MA* and *NHE*, can occur at different angles of mainshock and subsequent aftershocks as well.

(d) The results demonstrate considering the relative differences of consecutive incident angles in multiple earthquakes can lead to more critical structural responses. Therefore, it is necessary to rotate both mainshock and aftershocks by different angles for reliable seismic assessment of structures.

Declaration of Competing Interest

The authors declare that they have no known competing financial interests or personal relationships that could have appeared to influence the work reported in this paper.

References

[1] M. Araújo, L. Macedo, M. Marques, J.M. Castro Code-based record selection methods for seismic performance assessment of buildings. Earthquake Eng Struct Dyn 2016;45(1):129–148.

[2] S. Amiri, A. Soroushian A brief review on building structural analysis regulations in different seismic codes. Res Bull Seismol Earthquake Eng 2017;20(1):1–24. (in Persian).

[3] K. Goda, C.A. Taylor Effects of aftershocks on peak ductility demand due to strong ground motion records from shallow crustal earthquakes. Earthquake Eng Struct Dyn 2012;41(15):2311–2330.

[4] L. Di Sarno Effects of multiple earthquakes on inelastic structural response. Eng Struct 2013;56:673–681.

[5] S. Amiri, E. Bojórquez Residual displacement ratios of structures under mainshock-aftershock sequences. Soil Dyn Earthquake Eng 2019;121:179–193.

[6] L. Di Sarno, S. Amiri Period elongation of deteriorating structures under mainshock-aftershock sequences. Eng Struct 2019;196:109341.

[7] Amiri S, Garakaninezhad A, Bojorquez E. Normalized residual displacement spectra for post-mainshock assessment of structures subjected to aftershocks, Earthquake Engineering and Engineering Vibration (Accepted).

[8] J. Ruiz-García, J.C. Negrete-Manriquez Evaluation of drift demands in existing steel frames under as-recorded far-field and near-fault mainshock–aftershock seismic sequences. Eng Struct 2011;33(2):621–634.

[9] Y. Li, R. Song, J. Van de Lindt Collapse fragility of steel structures subjected to earthquake mainshock-aftershock sequences. J Struct Eng 2014;140(12):04014095.

[10] J. Ruiz-García, E. Bojorquez, E. Corona Seismic behavior of steel eccentrically braced frames under soft-soil seismic sequences. Soil Dyn Earthquake Eng 2018;115:119–128.

[11] A. Toorani, M. Gholhaki, R. Vahdani The investigation into the effect of consecutive earthquakes on the strongback bracing system. Structures 2020;24:477–488.

[12] M. Shokrabadi, H.V. Burton Risk-based assessment of aftershock and mainshock-aftershock seismic performance of reinforced concrete frames. Struct Saf 2018;73:64–74.

[13] E. Abraik Seismic performance of shape memory alloy reinforced concrete moment frames under sequential seismic hazard. Structures 2020;26:311–326.

[14] X. Guo, Z. He, J. Xu Identification of incremental seismic damage development in RC structures excited with sequence-type ground motions. Structures 2020;24:464–476.

[15] P. Oggu, K. Gopikrishna Assessment of three-dimensional RC moment-resisting frames under repeated earthquakes. Structures 2020;26:6–23.

[16] Tesfamariam S, Goda K, Energy-based seismic risk evaluation of tall reinforced concrete building in Vancouver, BC, Canada, under Mw9 megathrust subduction earthquakes and aftershocks, Frontiers in Built Environment (2017);3(29).

[17] R. Oyguc, C. Toros, A.E. Abdelnaby Seismic behavior of irregular reinforced-concrete structures under multiple earthquake excitations. Soil Dyn Earthquake Eng 2018;104:15–32.

[18] K. Goda Comparison of peak ductility demand of inelastic SDOF systems in maximum elastic response and major principal directions. Earthquake Spectra 2012;28(1):385–399.

[19] M. Torbol, M. Shinozuka The directionality effect in the seismic risk assessment of highway networks. Struct Infrastruct Eng 2014;10(2):175–188.

[20] J.C. Reyes, E. Kalkan Significance of rotating ground motions on behavior of symmetric-and asymmetric-plan structures: Part I. Single-story structures, Earthquake Spectra 2015;31(3):1591–1612.

[21] O. Taskari, A. Sextos Multi-angle, multi-damage fragility curves for seismic assessment of bridges. Earthquake Eng Struct Dyn 2015;44(13):2281–2301.

[22] D. Giannopoulos, D. Vamvatsikos Ground motion records for seismic performance assessment: To rotate or not to rotate? Earthquake Eng Struct Dyn 2018;47(12):2410–2425.

[23] K.G. Kostinakis, G.E. Manoukas, A.M. Athanatopoulou Influence of seismic incident angle on response of symmetric in plan buildings. KSCE J Civ Eng 2018;22(2):725–735.

[24] Y. Wang, L. Ibarra, C. Pantelides Effect of incidence angle on the seismic performance of skewed bridges retrofitted with buckling-restrained braces. Eng Struct 2020;211:110411.

[25] W. Wen, D. Ji, C. Zhai Ground motion rotation for mainshock-aftershock sequences: Necessary or not? Soil Dyn Earthquake Eng 2020;130:105976.

[26] M. Hatzivassiliou, G.D. Hatzigeorgiou Seismic sequence effects on three-dimensional reinforced concrete buildings. Soil Dyn Earthquake Eng 2015;72:77–88.

[27] F. Hosseinpour, A.E. Abdelnaby Effect of different aspects of multiple earthquakes on the nonlinear behavior of RC structures. Soil Dyn Earthquake Eng 2017;92:706–725.

[28] K. Kostinakis, K. Morfidis The impact of successive earthquakes on the seismic damage of multistorey 3D R/C buildings. Earthquakes Struct 2017;12(1):1–12.

[29] E. Omranian, A.E. Abdelnaby, G. Abdollahzadeh Seismic vulnerability assessment of RC skew bridges subjected to mainshock-aftershock sequences. Soil Dyn Earthquake Eng 2018;114:186–197.

[30] J. Ruiz-García, S. Yaghmaei-Sabegh, E. Bojórquez Three-dimensional response of steel moment-resisting buildings under seismic sequences. Eng Struct 2018;175:399–414.

[31] G. Wang, Y. Wang, W. Lu, P. Yan, M. Chen Earthquake Direction Effects on Seismic Performance of Concrete Gravity Dams to Mainshock-Aftershock Sequences. J Earthquake Eng 2018;1–22.

[32] Y. Yukutake, Y. Iio Why do aftershocks occur? Relationship between mainshock rupture and aftershock sequence based on highly resolved hypocenter and focal mechanism distributions, Earth. Planets and Space 2017;69(1):68.

[33] G. Rinaldin, C. Amadio, M. Fragiacomo Effects of seismic sequences on structures with hysteretic or damped dissipative behaviour. Soil Dyn Earthquake Eng 2017;97:205–215.

[34] G. Rinaldin, M. Fragiacomo, C. Amadio On the accuracy of the N2 inelastic spectrum for timber structures. Soil Dyn Earthquake Eng 2017;100:49–58.

[35] G. Rinaldin, C. Amadio Effects of seismic sequences on masonry structures. Eng Struct 2018;166:227–239.

[36] G. Rinaldin, M. Fasan, S. Noé, C. Amadio The influence of earthquake vertical component on the seismic response of masonry structures. Eng Struct 2019;185:184–193.

[37] W. Wen, D. Ji, C. Zhai Cumulative Damage of Structures under the Mainshock-aftershock Sequences in the Near-fault Region. J Earthquake Eng 2020;1–15.

[38] X.-H. Yu, S. Li, D.-G. Lu, J. Tao Collapse Capacity of Inelastic Single-Degree-of-Freedom Systems Subjected to Mainshock-Aftershock Earthquake Sequences. J Earthquake Eng 2020;24(5):803–826.

[39] D. Giannopoulos, D. Vamvatsikos, Influence of rotated ground motion components on the response distribution of inelastic oscillators, in: 5th International Conference on Computational Methods in Structural Dynamics and Earthquake Engineering Methods in Structural Dynamics and Earthquake Engineering (COMPDYN 2015), Crete Island, Greece, 2015.

[40] Pacific Earthquake Engineering Research Center. PEER ground motion database (https://ngawest2.berkeley.edu/).

[41] P. Fajfar Capacity spectrum method based on inelastic demand spectra. Earthquake Eng Struct Dyn 1999;28(9):979–993.